

Study the effect of welding parameters on the mechanical properties and microstructure of aluminum alloy (5052)

Mohamed. R. Budar

Abdel hafid. B. Kridan

Akrm Almabrouk Ali Alaya

Hamza Abobakr O Ali

Almumonu2013@gmail.com

Abstract:

The Gas Tungsten Arc Welding process of aluminum alloys is an important industrial technology but many challenges remain. The objective of this paper is to investigate the effect of TIG welding parameters on the depth of penetration of the given specimen and also on the quality of the lap welded AA5052 aluminum alloy. The influences of the heat input, welding speed and gas flow rate on the mechanical and micro hardness properties of the joints were experimentally investigated. The mechanical properties of the joints were evaluated by performing tensile tests. From the experimental results, optimum process parameters were determined, and microstructural examination and micro hardness tests were conducted to better understand the performance of the joints. It was found that there is a correlation between the tensile shear loads of the joints and heat input per unit length. At the optimized parameters, the welded joint showed good weld appearance without macro defects, and the joint had an adequate tensile

Keywords: AA5052, Gas Tungsten Arc Welding, mechanical properties, micro-hardness, microstructure.

1.Introduction

Due to their distinguishable advantages aluminum alloys are widely applied in the shipbuilding, aerospace, as well as automotive industries. [1].

The aluminum and copper alloys are difficult to weld due to their high thermal conductivity, high thermal expansion and tendencies to produce porous welds⁸. The high thermal conductivity means that there is a high rate of cooling and so there is difficulty in heating up the parent metal round the weld zone to a high enough temperature to give complete fusion with the weld pool [2]. Additionally, the high coefficient of expansion means that significant residual stresses are produced due to expansion being constrained by the colder surrounding parent metal. Moreover, porosity arises because the metal in the molten state absorbs hydrogen from the sources as the welding flame, fluxes and atmospheric moisture and when the weld cools, this hydrogen is released [3].

Tungsten Inert Gas Welding (TIG) is often done by melting the work pieces and adding a filler material to form a pool of molten material (the weld pool) that cools to become a strong joint, with pressure sometimes used in conjunction with heat, or by itself, to produce the weld. This is in contrast with soldering and brazing, which involve melting a lower-melting-point material between the work pieces. Only in this way can the designer use most suitable materials for each part of a given structure [4]. The growing availability of new materials and higher requirements being placed on materials and the welding processes. Gas tungsten arc welding, also known as

tungsten inert gas (TIG) welding, produces an arc between a tungsten electrode and work piece. An inert gas shields the arc, electrode, and molten pool from atmospheric contamination. When welding thinner materials, edge joints, and flanges, welders generally do not use filler metals. However, for thicker materials, welders primarily use externally fed filler metal. TIG welding is a popular technique for joining thin materials in the manufacturing industries.

Generally, the quality of a weld joint is directly influenced by the welding input parameter settings, though selection of proper process parameters is important to obtain the desired weld bead profile and quality [5].

In this paper the effect of the TIG welding parameters such as welding Current, welding Speed, gas flow rate and heat input) on the mechanical properties and microstructure of the weld have been investigated.

2.literature Review:

Penetration is considered as one of the most important properties of a weld, since it determines the stress carrying capacity of the welded joint [16]. It represents the maximum linear distance

Ancona et al [6] conducted laser butt welding of AA5083 aluminum alloy. They used the design of the experiment technique to investigate the effects of the variables on the mechanical properties and porosity level and stated that in terms of tensile load the best results were found for high powers and high welding speeds.

Narayanan et.al [7] found out the Influence of Gas Tungsten Arc Welding Parameters in Aluminum 5083 Alloy welding with different flow rate of gas and different welding current 200 and 250A. After welding, tensile testing, Micro hardness testing and Macrostructure and Microstructure study tests was done on specimen. From this study it was shown that maximum ultimate strength is 281MPa, hardness of weld metal is 73.5 HVN at welding current 200A and gas flow rate 15 LPM.

Hussain et.al [8] investigated the effect of welding speed on tensile strength of the welded joint by TIG welding process of AA6351 Aluminum alloy of 4 mm thickness. Welding was done on specimens of single V butt joint with welding speed of 1800 -7200 mm/min. From the experimental results it was revealed that strength of the weld zone is less than base metal and tensile strength increases with reduction of welding speed.

2. Experimental Procedure

2.1 Welding machine:



Fig. 1: TIG Welding Machine **Fig. 2:** Argon gas cylinder **Fig. 3:** Welding Torch

2.2 Gas Cylinder

Gas cylinder- for TIG welding argon gas is supplied to the welding torch with a particular flow rate so that an inert atmosphere formed and stable arc created for welding. Gas flow is control by regulator and valve

2.3 Welding Torch

TIG and Torches Feature Silicone Rubber torch bodies to reduce accidental damage during use the loss of high frequency signal due to torch body cracking related to hard body plastic torch.

2.4 Welding parameters

- A. **Welding Current**, It controls the melting rate of the electrode and thereby the weld deposition rate. It also controls the depth of penetration and thereby the extent of dilution of the weld metal by the base metal.
- B. **Welding Speed and Heat input** Welding speed is the linear rate at which the arc moves with respect to plate along the weld joint. Welding speed generally conforms to a given combination of welding current and voltage. If welding speed is more than required heat input to the joint decreases, less filler metal is deposited than required, Reinforcement height decreases'. If welding speed is slow, heat input rate increases, Weld width increases and reinforcement height also increases more convexity [9].
- C. **Gas flow rate** argon is the most used GTAW shielding gas. Argon is used in welding of carbon and stainless steels and low thickness aluminum alloys components. Gas flow rate influence the welding speed and improves process tolerance. Heat input rate= $60VI/v$ J/mm
 V =arc voltage in volts I =welding current in ampere, v =speed of welding in mm/min

2. Materials and Experimental Procedures

2.1. Materials

The Al-alloy (5052) of 350mm long x 50mm wide x 6 mm thick was under investigation. The chemical composition of AA5052 is shown in Table.1.

Table 1: Chemical Composition of aluminum alloy (5052)

| Chemical composition %wt |
|--------------------------|
|--------------------------|

| material | Si | Fe | Cu | Mn | Mg | Zn | Ti | Cr | Al |
|---------------|-----|-----|-----|-----|-----|-----|-----|------|---------|
| Al alloy 5052 | 0.6 | 0.5 | 0.1 | 0.5 | 2.6 | 0.2 | 0.1 | 0.25 | Balance |

The filler wire of ER4043 grade was utilized for welding all the specimens because of its good, mechanical and physical properties which are similar to the base metal. The chemical composition of ER4043 filler wire is shown in table 2.

Table 2: Chemical Composition of ER4043 Filler Wire

| Chemical composition %wt | | | | | | | |
|--------------------------|-------|-----|-----|------|------|-----|-----|
| material | Si | Fe | Cu | Mn | Mg | Zn | Ti |
| ER4043 | 4.5-6 | 0.8 | 0.3 | 0.05 | 0.05 | 0.1 | 0.2 |

2.2 Tensile test:

Tensile test of the welded joint was performed with universal tensile testing machine (ZWICK 1000) connected to computer to draw the stress-strain curves and recording the tensile strength. Tensile test was carried out according to ASTM B57 and Test were performed at room temperature.

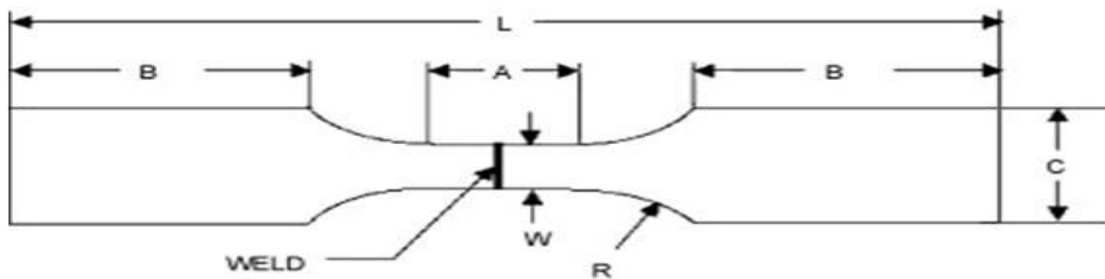


Fig. 4 ASTM B57 Testing specimen

In this experimental work TIG welding is used to weld 5052 aluminum alloy with use of 4043 graded filler wire. Nine specimens of dimensions 100 mm long x 50 mm width x 6 mm thick are prepared, then weld each two specimens and form nine number of butt weld joints, welded specimen is shown below in figure 5: Before welding, edges of the work pieces are suitably prepared. The edges are cleaned of dust using wire brush and cloths.



Fig. 5: specimen of welded aluminum alloy 5052

Table 3: Dimension of the Tensile Test Specimen

| Name | Dimensions (mm) |
|------|-----------------|
| L | 350 |
| A | 50 |
| W | 20 |
| R | 25 |
| B | 90 |
| C | 35 |
| T | 6 |

Current = 130,150 and 170, Amp were applied. The terminal voltage was 20 V and gas flow rate was varied during the welding. Welding speed was calculated for each welded specimen. Upon finishing the welding processes, and in order to measure the depth of penetration, welds were cut perpendicular to the direction of welding on power hacksaw, then with the help of measuring instrument, depth of penetration of welded specimens was measured.

In this paper, heat input is calculated for each welded specimen by the mathematical formula:

Heat input or Energy is calculated from mathematical formula:

Heat input (joule/mm) = $60 VI/S$.

Where,

V = Arc voltage in volt

I = Welding current in ampere

S = Welding speed in mm/min.

3.Results and discussion

Readings of depth of penetration obtained by measuring instrument after cutting each specimen perpendicular to weld bead direction and the values of depth of penetration with respect to input parameters such as welding speed, gas flow rate and heat input are listed in Table 3

Table 3: Depth of penetration of welded specimen for the experiment.

| Specimen ID | Welding Current (Amps) | Arc Voltage (V) | Arc Time (Sec.) | Welding Speed (mm/Min.) | Gas Flow Rate (Lt/Min.) | Heat Input (J/mm) | Depth of Penetration (mm) |
|-------------|------------------------|-----------------|-----------------|-------------------------|-------------------------|-------------------|---------------------------|
| 1 | 130 | 20 | 39 | 66 | 10 | 2364 | 5.38 |
| 2 | 130 | 20 | 45 | 78 | 11 | 2000 | 5.42 |
| 3 | 130 | 20 | 33 | 90 | 12 | 1733 | 5.48 |
| 4 | 150 | 20 | 31 | 96 | 11 | 1875 | 5.56 |
| 5 | 150 | 20 | 25 | 102 | 12 | 1765 | 5.62 |
| 6 | 150 | 20 | 32 | 120 | 10 | 1500 | 5.73 |
| 7 | 180 | 20 | 21 | 134 | 12 | 1612 | 5.83 |
| 8 | 180 | 20 | 21 | 144 | 10 | 1500 | 5.88 |
| 9 | 180 | 20 | 19 | 156 | 11 | 1385 | 5.93 |

The depth of penetration increases with welding increases speed up to 96 mm/min which was optimum value to obtain maximum penetration, because it begins to increases linearly after this point. Increasing the speed of travel and maintaining constant arc voltage and current increases penetration until an optimum speed 156 mm/min is reached at which penetration is maximum 5.93 mm. Increasing the speed beyond this optimum result in increases penetration and maximum depth of penetration occurs at heat input rate of 1385J/mm. Obviously, the greater the depth of penetration, the better of the weldability. Concluding the optimum weldability can be achieved by applying welding speed, 96 mm/min with current 150 Amp, arc voltage 20 V and gas flow rate 11Lt/mm.

3. 1 Effect of welding current on Depth of Penetration

Figure 6 (a) clearly describes that as increasing of welding current, the depth of penetration increases until an optimum value which gives maximum depth of penetration. The depth of penetration begins to decrease linearly after that optimum value. Therefore, maximum penetration of 5.93 mm is obtained for specimen 9 at welding current of 180 Amp.

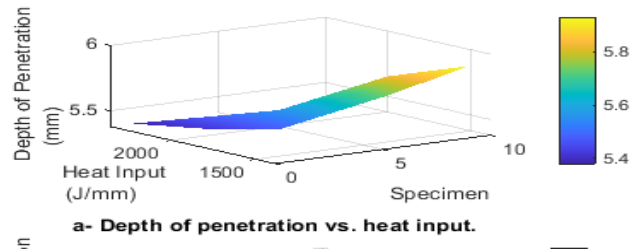


Fig. 6 (a). Depth of penetration Vs. heat input

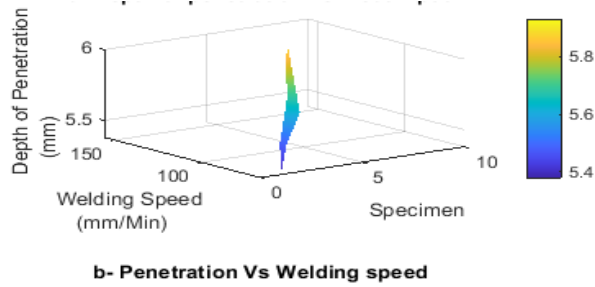


Fig. 6 (b). Penetration Vs. welding speed

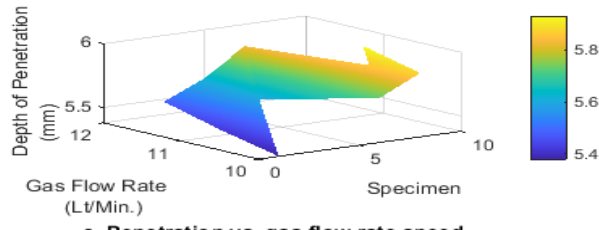


Fig. 6 (c). Penetration Vs. gas flow rate

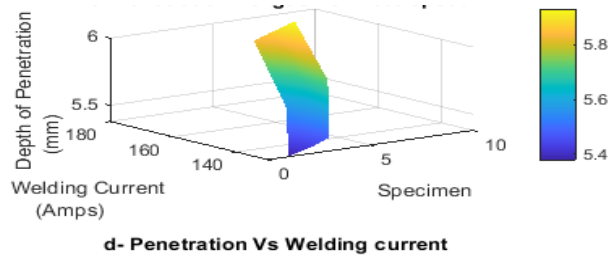


Fig. 6 (d) Penetration Vs. welding current

3.2. Effect of Welding Speed on Depth of Penetration

Figure 6 (b) illustrate the penetration resulted from varying of welding speed. It is clear from Figure 6 (b) that describes the depth of penetration increases linearly by increasing welding speed until an optimum value of maximum penetration equal to 5.93mm, the depth of penetration started to increase linearly. Therefore, maximum penetration of 5.93 mm was obtained for specimen (9) at welding speed of 156 mm/min.

3. 3 Effect of Gas Flow Rate on Depth of Penetration

The figure 6 (c) clearly describe that increasing gas flow rate, caused increase in the depth of penetration. The case was vailed up to 12Lt/mm which gave the maximum depth of penetration. Afterward, the depth of penetration starts to increase linearly. To conclude the maximum penetration of 5.93 mm was obtained from specimen 9 at gas flow rate of 11 Lt/min.

3. 4 Effect of Heat Input on Depth of Penetration

Figure 6(d) demonstrate the relationship between drawn between heat input and depth of penetration. It is obvious that as heat input increased the depth of penetration increased and the case was vailed up to the value of 5.93mm which gives maximum depth of penetration. Afterward, the depth of penetration began increasing linearly. The maximum depth of penetration of 5.93 mm for specimen 9 at heat input of 1385 J/mm.

3.5 The effect of welding current and speed on welding width.

Welding width for all the specimens were measured and calculated average welding width as shown in table 4. Average value of welding width then plotted against the welding speed for different welding current as shown in figure 7.

Table 4: Weld width for the first experiment.

| Sample | 1 | 2 | 3 | 4 | 5 | 6 | 7 | 8 |
|------------------------|------|------|------|------|------|------|------|------|
| average of width 1(mm) | 2.23 | 1.76 | 1.66 | 1.86 | 1.77 | 2.10 | 2.10 | 1.23 |

Figure 7: welding width of the samples with different welding speed and welding current.

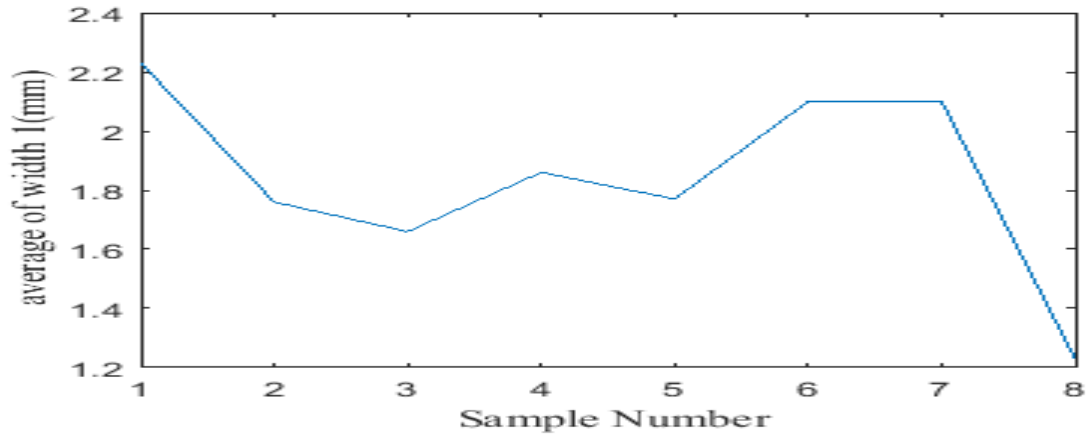


Figure 7, demonstrate the relationship between welding width and welding speed. It is obvious that as welding speed increased. The welding width decreased with an exception of value of 1.83mm until the value reached the welding width of 2.03mm. After this value, welding width begins to increase until value of 1.23mm. Therefore, maximum welding width of 2.23 mm is obtained for specimen 2 at welding speed of 66 mm/min.

3.6 The effect of welding parameters on tensile strength.

The table (5) illustrate the results which have been obtained from the experiment of the tensile strength and micro-hardness tests applying different welding current, welding speed and gas flow rate.

Table 5: Illustrate tensile test and micro-hardness test results

| Specimen number | Welding Current (Amps) | Welding Speed (mm/Min.) | Gas Flow Rate (Lt/Min.) | Micro-hardness test | Tensile test: MPa |
|-----------------|------------------------|-------------------------|-------------------------|---------------------|-------------------|
| 1 | 120 | 66 | 10 | 60.5 | 252.1 |
| 2 | 120 | 78 | 11 | 69.2 | 264.4 |
| 3 | 120 | 90 | 12 | 72.8 | 254.4 |
| 4 | 140 | 96 | 11 | 59.8 | 269.0 |

| | | | | | |
|---|-----|-----|----|------|----------|
| 5 | 140 | 102 | 12 | 87.2 | 255.5 |
| 6 | 140 | 120 | 10 | 64.5 | 260.7 |
| 7 | 160 | 144 | 12 | 57.7 | Fracture |
| 8 | 160 | 144 | 10 | 80.5 | 270.6 |
| 9 | 160 | 156 | 11 | 59.3 | 280.4 |
| | | | | | |

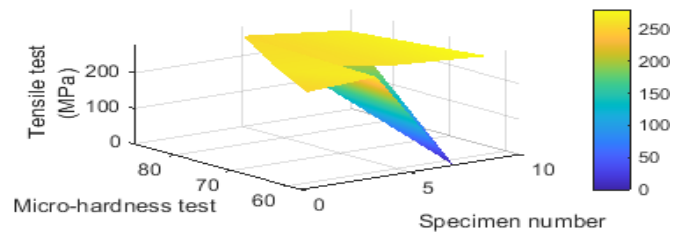


Fig. 8: Tensile strength Vs micro-hardness

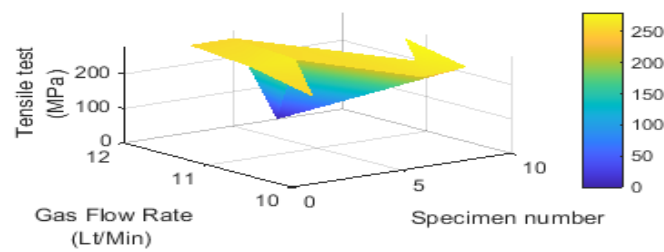


Fig. 9: Tensile strength against gas flow rate

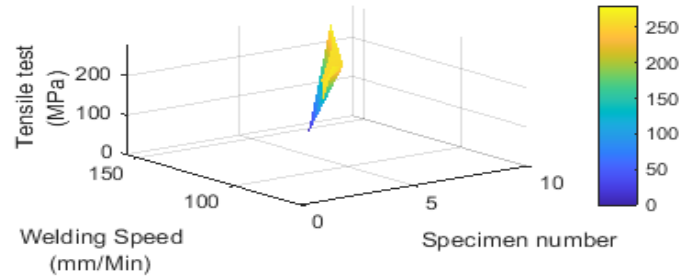


Fig. 10: Tensile strength against welding speed

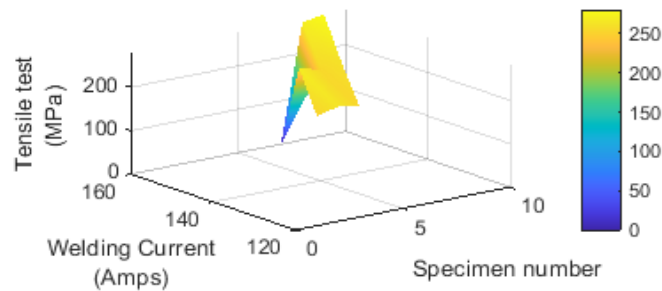


Fig. 11: Tensile strength against different welding current

The tensile tests were conducted on the TIG weld specimens to study the tensile properties, and the results are reported in figure 8. The stress-strain curve of 5052 aluminum alloy and weldments is illustrated in figure 9, which shows the yield and tensile strength data. The average tensile strength, yield strength, and elongation of base metal 5052 were tested and reported to be 254.4 MPa, 280.4 MPa, and 22%, respectively. Figure 10, figure 11 shows the tensile tested of the welded specimens after a fracture. The fracture location of the weld tensile specimens was in weld FZ due to the microstructure of the fusion welding process and the formation of coarse grains due to high welding heat and porosities. The common welding defects such as porosities in weld FZ could be the reason for crack initiation during tensile testing when failure is found in the FZ. The fracture location of the tensile test samples welded specimens was identified at the HAZ, in between the FZ and BM region

The strength of the weld joint was not able to reach up to BM due to the effect of heat beside the fusion zone, causing it to lose strain hardened effect of the BM.

3.7. The effect of welding parameters on micro hardness.

The hardness investigation was studied on the weld specimens in the transverse direction, from Fusion Zone (FZ) to the base material region, and the hardness profile was shown in figure 12.

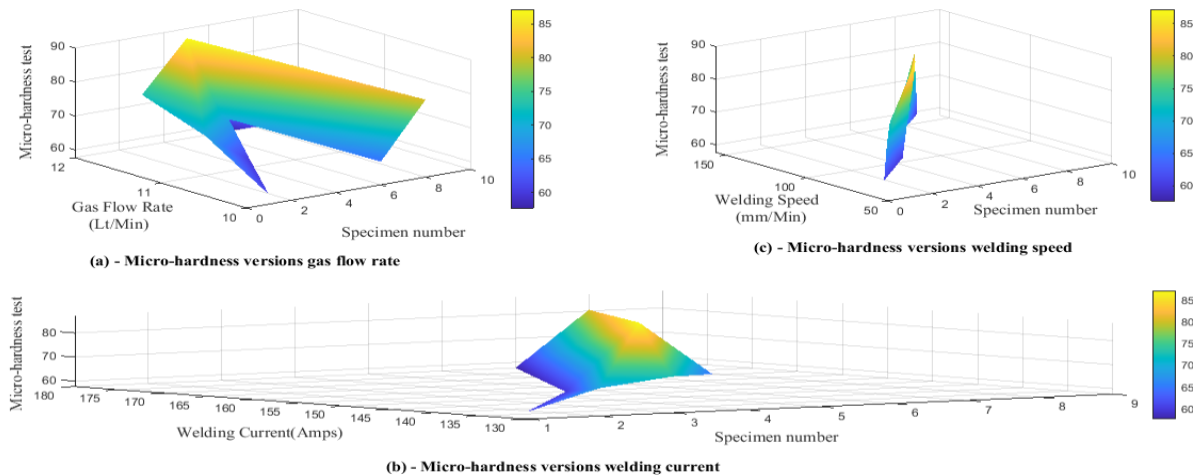


Fig. 12: Micro-hardness value from the center of the weld zone towards the base material for welding done with different welding speed and different welding current.

. The average hardness value of base metal AA5052 was obtained at 73HV. During the TIG weldment, severe plastic deformation was induced by the generation of frictional heat. This might be altering the weld bead microstructure, grain refinement in the stirred zone. Therefore, the hardness of the welded zone was increased, which contributes to enhancing the strength of the TIG treated weldment. The hardness values were noticed to be less due to coarse particles, microstructure, and the evaporation of Mg elements by the effect of the thermal cycle during fusion welding. Typically the coarse particle microstructure in Al-Mg alloys results in lower hardness measurements. However, the weld zone exhibits a higher hardness than the base metal, using ER4043 filler. The hardness increases with the inclusion of Mg content in aluminum alloys. The hardness was increased due to the development of hardening intermetallic phases like Al_3Mg_3 in FZ with the dilution of higher Mg content into Al alloy. These intermetallic phases are responsible for high hardness in the FZ relative to the base metal. The decline in hardness value towards the HAZ location is due to the loss of strain hardening effect, and grain coarsening is caused by the thermal cycle during fusion welding. Hardness reduction in HAZ region due to grain coarsening of strengthening particles. The hardness plot clearly shows the marginal improvement of hardness in the processed zone. Furthermore, the higher hardness in a few locations of FZ is the result of the formation of hard intermetallic phases.

5. Microstructural

The microstructure of the aluminum alloy 5052 is shown in figures 13, 14, 15 respectively. They seem that there is a difference in the grain size of both of weld metal (WM) and heat affected zone (HAZ). The grain size may be one of a factor that can be considered can affect the mechanical properties of aluminum alloys.

No recrystallization phenomena can be observed in these situations of the HAZ. This is because the temperature caused by the TIG welding process is insufficient and the deformation is not so severe to cause recrystallization. However, the shapes of grains in the HAZ reveal an obvious

reduction in sizes and the density of distribution. In the weld metal WM, the grains become larger gradually.

SEM image of the base metal figure 13 shows that the particles are marginally stretched in the rolling direction and are in irregular size, color, and shape, attributed to the cold rolling process. SEM image of 5052 alloy shows that β -phase particles were homogeneously distributed on Al matrix. Figure 14 displays the appropriate TIG weld fusion zone without processing. It shows the smaller particles with a straight shape after the solidification. In the TIG weld fusion zone, the distribution of particles was homogeneous, as the material is melted to high temperature and re-solidified quickly. The number of particles visible was higher due to higher Mg content in ER 4043 filler rod. The impact of TIG is displayed in figure 15, where the weld bead was processed.

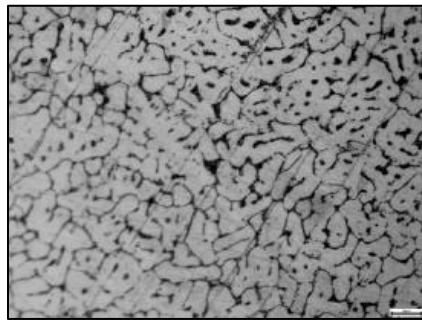


Fig. 13: Micrographs at the cross section of the welding done with different
Welding speed for welding current of 130 A

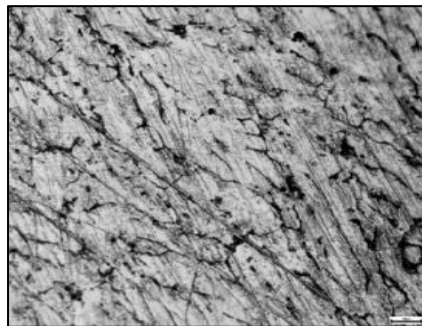


Fig. 14: Micrographs at the cross section of the welding done with different
Welding speed for welding current of 150 A

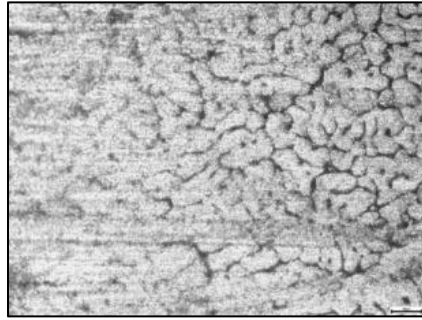


Fig. 15: Micrographs at the cross section of the welding done with different Welding speed for welding current of 170 A

7. Conclusion

A new methodology has been explored to assess the effort of TIG-welded AA5052 plates with ER4043 filler rod. This strategy has shown to be effective, as seen by the conclusions listed below.

The microstructure and mechanical characteristics of the TIG weldment have been enhanced, and the porosities are eliminated.

The TIG illustrates the fine recrystallization of particles due to stirring action, which could improve the mechanical properties of the welded joints.

The mechanical properties of TIG-welded joints have been improved. The maximum tensile strength value was 280.4 MPa.

The hardness TIG welded joints has a marginal increase.

The implementation of TIG welding process has enhanced the ductility of the welded joints as the failure location was away from the weld fusion zone. The ductility of welded joints is linked with the surface morphology observations, which are defect-free and have smaller dimples sizes.

The effect of weld bead was minimum considering the weld plate thickness; however, it has considerably improved the mechanical characteristics of TIG-welded joints

References

1. Tu, J.F.; Paleocrassas, A.G. Fatigue crack fusion in thin-sheet aluminum alloys AA7075-T6 using low-speed fiber laser welding. *J. Mater. Process. Technol.* 2011, volume 211, page 95–102.
2. Jeyaprakash N, Adisu H and Arunprasath M. “The Parameters and Equipment Used in TIG Welding: A Review” *The International Journal of Engineering and Science (IJES)* Volume 4 Issue 2, 2015, pp.11-20.
3. Khann OP. A Textbook of welding technology. New Delhi: Dhapat Rai. laser welding. *Mater. Sci. Eng. A* 2007, volume 447, page 197–208.
4. Thakur Y, Kumar K and Kumar K “Influences of TIG welding parameters on tensile and impact behavior of aluminum alloy joints: A Review”, *IOSR Journal of Mechanical and Civil Engineering (IOSR-JMCE)*, Special Issue - AETM'16, 2016, pp. 54-58.
5. Kumar A. and Sundarrajan S “Optimization of pulsed TIG welding process parameters on mechanical properties of AA 5456 Aluminum alloy weldments,” *Materials and Design* 30, 2009, pp. 1288–1297.
6. Ancona, A., Lugara, P.M., Sorgente, D., Tricarico, L. (2007). Mechanical characterization of CO2 laser beam butt welds of AA5083. *Journal of Materials Processing Technology*, vol. 191, no. 1-3, p. 381-384, DOI: 10.1016/j.jmatprotec.2007.03.048.
7. Narayanan A, Mathew C, Yeldo B V and Joseph J, “ Influence of Gas Tungsten Arc Welding Parameters in Aluminium 5083 Alloy” *International Journal of Engineering Science and Innovative Technology (IJESIT)*, Volume 2, Issue 5, September 2013, pp. 269-277.
8. Hussain A. K., Lateef A., Javed M., and Pramesh T. “Influence of Welding Speed on Tensile Strength of Welded Joint in TIG Welding Process,” *International Journal of Applied Engineering Research*, Dindigul, 1, 2010 pp. 518-527.